Journal of Navigation and Port Research International Edition
Vol.32, No.7 pp. 543~552, 2008 (ISSN-1598-5725)

Wave Force Analysis of the Three Vertical Cylinders in Water Waves

Nam-Hyeong Kim† · *Tan Ngoc Than Cao**

† *Major of Civil and Environmental Engineering, Cheju National University, Jeju, Korea, 690 756*
**Graduated School, Cheju National University, Jeju, Korea, 690-756*

Abstract : *The diffraction of waves by three bottom fixed vertical circular cylinders is investigated by using the boundary element method. This method has been successfully applied to the isolated vertical circular cylinder and now is used to study the interaction between waves and multiple vertical cylinders. In this paper, a numerical analysis by the boundary element method is developed by the linear potential theory. The numerical analysis by the boundary element method is based on Green's second theorem and introduced to an integral equation for the fluid velocity potential around the vertical circular cylinders. To verify this method, the results obtained in present study are compared with the results computed by the multiple scattering method. The results of the comparisons show strong agreement. Also in this paper, several numerical examples are given to illustrate the effects of various parameters on the wave exciting force such as the separation distance, the wave number and the incident wave angle. This numerical computation method might be used broadly for the design of various offshore structures to be constructed in the future.*

Key words : *Diffraction of waves, Boundary element method, Three vertical circular cylinders, Green's second theorem, Wave force, Run up.*

1. Introduction

Recently, a number of large offshore structures, such as a large-scale offshore airport or work station, have been constructed with several elementary members or legs such as cylinders. Thus, the interactions between waves and a group of cylinders need to be investigated for accurate theoretical predictions, and much work has been done on this subject in recent years. Spring and Monkmeyer (1974) obtained a solution interaction among two arbitrary cylinders in water waves. Kagemoto and Yue (1986) combined the direct matrix method and the multiple scattering technique to obtain an exact algebraic method. After these researches, many theories that analyze the interaction between waves and number of cylinders were suggested (Chakrabarti, 2000; Kim, 1992; Williams and Li, 2000).

There are many previous studies on piles with boundary element method. Notably, based on the linear diffraction theory, the wave force analysis of the vertical circular cylinder by boundary element method was studied by Kim and Park (2007), and its numerical results by boundary element method were strong agreement with those of MacCamy and Fuchs (1954).

In this paper, a practical method of boundary element method for calculating wave force acting on three vertical cylinders is presented. The wave force analysis method based on Green's second theorem in indirect boundary element method using linear velocity potential theory is developed. To verify this method, the wave forces acting on three vertical circular cylinders obtained in present numerical method are compared with those of Han and Ohkusu (1995), Chakrabarti (1978). The comparisons show that the results of present study have strong agreement with their results. Also in this paper, several numerical examples are given to illustrate the effects of various parameters on the wave exciting force such as the separation distance, the wave number and the incident wave angle. The run-up and free-surface elevation around three vertical circular cylinders group are also investigated.

2. Basic Equations

2.1 Formulation of problem

The interaction of linear waves with three bottom-fixed vertical cylinders is investigated in this paper. Three vertical circular cylinders, having radius a, are arranged in the water of uniform depth h. The global Cartesian coordinate system (x,y,z) is defined with the origin located at the center of the geometry and on the still-water level, the z axis directed vertically, x and y axis directed

† Corresponding Author: Nam-hyeong Kim, nhkim@cheju.kr 064) 754 3453
* ctnthan@cheju.ac.kr 064) 754-3453

horizontally. The geometry of this problem is shown in Fig. 1.

As usual, it is assumed that the fluid is inviscid, incompressible, its motion is irrotation, and fluid motion is small. The structure subjected to a strain of regular surface wave of height H and the angular frequency σ propagating at an angle β to the positive x axis. The velocity potential Φ can be defined by:

$$\Phi(x,y,z,t) = R_e[-i\frac{g}{\sigma}\frac{H}{2}\phi(x,y,z)e^{-i\sigma t}] \tag{1}$$

where $R_e[]$denotes the real part of complex expression.

From the linear feature of the potential flow, the total velocity potential in equation (1) is a sum of incident wave velocity potential and scattered (reflected plus diffracted) wave velocity potential and is defined as follows:

$$\phi = \phi_i + \phi_s \tag{2}$$

$$\phi_i = \frac{\cosh k(h+z)}{\cosh kh}\Psi_i;\quad \Psi_i = e^{ik(x\cos\beta + i\sin\beta)} \tag{3}$$

where ϕ_i and ϕ_s are incident wave velocity potential and scattered wave velocity potential, respectively. $H/2$ is wave amplitude, g is acceleration due to gravity, and the wave number k is the positive real root of the dispersion relation:

$$\sigma^2 = gk\tanh kh \tag{4}$$

Boundary value problems by the formulation of scattered wave velocity potential ϕ_s are given as follows:

- Laplace equation:

$$\nabla^2\phi_s = 0 \text{ in } \Omega \tag{5.a}$$

- Free surface boundary condition:

$$\frac{\partial\phi_s}{\partial z} - \frac{\sigma^2}{g}\phi_s = 0 \text{ on } \Gamma_F \tag{5.b}$$

- Cylinder surface boundary condition:

$$\frac{\partial\phi_s}{\partial n} = -\frac{\partial\phi_i}{\partial n} \text{ on } \Gamma_{H_m},\ m=1,2,3 \tag{5.c}$$

- Sea bed boundary condition:

$$\frac{\partial\phi_s}{\partial z} = 0 \text{ on } \Gamma_B \tag{5.d}$$

- Radiation boundary condition:

$$\lim_{R\to\infty}\sqrt{R}\left\{\frac{\partial\phi_s}{\partial R} - ik\phi_s\right\} = 0 \text{ on } \Gamma_R \tag{5.e}$$

where Ω is fluid region, Γ_F is free surface, Γ_{H_m}, $m=1,2,3$ is the body surface of cylinder 1, cylinder 2 and cylinder 3 respectively, Γ_B is the sea bed, i is the imaginary unit $i=\sqrt{-1}$, and Γ_R is virtual boundary at infinity and $R=\sqrt{x^2+y^2}$.

The scattered wave velocity potential ϕ_s are defined as follows

$$\phi_s = \frac{\cosh k(h+z)}{\cosh kh}\Psi_s(x,y) \tag{6}$$

If the definitions of equation (3) and (6) are substituted into equations (5.a)~(5.e), the boundary value with Ψ_s are obtained as follows:

$$\nabla^2\Psi_s + k^2\Psi_s = 0 \text{ in } \Omega \tag{7.a}$$

$$\frac{\partial\Psi_s}{\partial n} = -\frac{\partial\Psi_i}{\partial n} \text{ on } \Gamma_{H_m},\ m=1,2,3 \tag{7.b}$$

$$\lim_{R\to\infty}\sqrt{R}\left\{\frac{\partial\Psi_s}{\partial R} - ik\Psi_s\right\} = 0 \text{ on } S_\infty \tag{7.c}$$

The quantity n is the direction normal at the structure surface and defines the outward normal to a panel on the surface cylinder.

In equations (7.a)~(7.c) boundary value problems are two dimensional problems of $x-y$ plane shown in Fig. 2. Finally, by analyzing boundary value problem by Ψ_s , the scattered wave velocity potential is determined, and wave pressure and wave force acting on cylinders are calculated by using it.

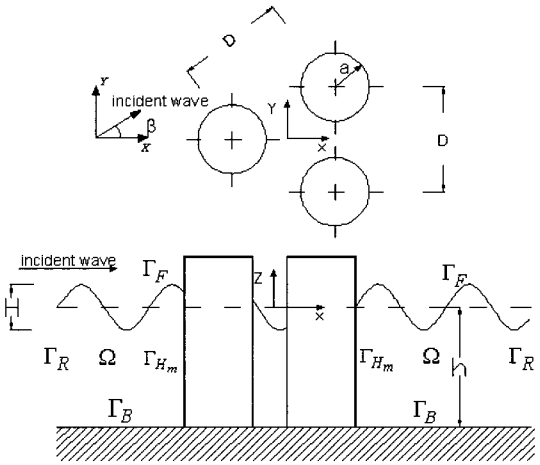

Fig. 1 Definition of three vertical circular cylinders

2.2 Formulation of Boundary Element Method

The fundamental solution G of the Helmholtz equation is defined by:

$$\nabla^2 G + k^2 G + \delta(x-\xi, y-\eta) = 0 \tag{8}$$

where δ is Dirac Delta function. G is the fundamental solution for Helmholtz equation:

$$G = \frac{i}{4} H_0^{(1)}(kr) \tag{9}$$

where $r = \sqrt{(x-\xi)^2 + (y-\eta)^2}$; $(\xi,\eta)$and (x,y) are the coordinate of the source point and observation point respectively. The $H_0^{(1)}(kr) = J_0(kr) + i\,Y_0(kr)$is the Hankel function of the first kind of order zero. If the observation point i is presented over boundary S plan, the boundary value problems of Eqs. (8.a)~(8.c) are defined by integral equation as Eq. (11):

$$\frac{1}{2}\Psi_{si} + \int_{S_H + S_{H_1} + S_{H_2} + S} \Psi_s \frac{\partial G}{\partial n} ds = \int_{S_H + S_{H_1} + S_{H_2} + S_\infty} \frac{\partial \Psi_s}{\partial n} G ds \tag{10}$$

where $S_\infty : R \to \infty$ is shown by closed curve with circular shape in a virtual boundary plane in Fig. 2.

If observation point i is near S_{H_m}, the Eq. (10) is the integral equation for S_∞. When S_∞ is near $S_{H_m}$with $r \gg 1$, $kr \cong r$, $r \cong R$, the Hankel functions are given as follows:

$$\left.\begin{aligned} H_0^i(kr) &\cong \sqrt{\frac{2}{\pi kR}}\, e^{i(kR - \frac{\pi}{4})} \\ \frac{\partial H_0^i(kr)}{\partial n} &\cong ik\sqrt{\frac{2}{\pi kR}}\, e^{i(kR - \frac{\pi}{4})} \end{aligned}\right\} \quad \text{on } S_\infty \tag{11}$$

The integral term for S_∞ of Eq. (10) is substituted as follows:

$$\begin{aligned} &\int_{S_\infty} \Psi_s \frac{\partial G}{\partial n} ds - \int_{S_\infty} \frac{\partial \Psi_s}{\partial n} G ds \\ &= \frac{1}{4i}\sqrt{\frac{2}{\pi k}}\, e^{-i\frac{\pi}{4}} \int_{S_\infty} \frac{e^{ikR}}{\sqrt{R}} \left(\frac{\partial \Psi_s}{\partial R} - ik\Psi_s \right) ds \\ &= \frac{1}{4i}\sqrt{\frac{2}{\pi k}}\, e^{-i\frac{\pi}{4}} \int_0^{2\pi} e^{ikR} \sqrt{R} \left(\frac{\partial \Psi_s}{\partial R} - ik\Psi_s \right) d\theta \end{aligned} \tag{12}$$

By, substituting Eq. (12) into Eq. (7c), the resulting is as follows:

$$\int_{S_\infty} \Psi_s \frac{\partial G}{\partial n} ds - \int_{S_\infty} \frac{\partial \Psi_s}{\partial n} G ds = 0 \tag{13}$$

Therefore, the final boundary integral equation on scattered wave potential is given as follow:

$$\frac{1}{2}\Psi_{si} + \int_{S_H + S_{H_1} + S_{H_2}} \Psi_s \frac{\partial G}{\partial n} ds = \int_{S_{H_1} + S_{H_2} + S_{H_3}} \frac{\partial \Psi_s}{\partial n} G ds \tag{14}$$

Eq. (14) is the integral equation for the near curve S_{H_m}, $m = 1,2,3$ of the cylinder surface.

The scattered wave velocity potential is derived by solving the Eq. (14). Once the incident wave velocity potential and scattered wave velocity potential are known, then the pressure and the wave forces on each cylinders can be computed. The scattered wave potential in the domain Ω can be obtained after the scattered wave potential on the boundary has been calculated. If the observation point i is placed in the domain Ω, the integral equation for scattered wave potential in the domain Ω is given as follow:

$$\Psi_{si} = \int_{S_{H_1} + S_{H_2} + S_{H_3}} \frac{\partial \Psi_s^e}{\partial n} G ds - \int_{S_{H_1} + S_{H_2} + S_{H_3}} \Psi_s^e \frac{\partial G}{\partial n} ds \tag{15}$$

where Ψ_s^e, $\frac{\partial \Psi_s^e}{\partial n}$ are the scattered wave potential and the normal derivative of the scattered wave potential on the boundary S_{H_1}, S_{H_2}, and S_{H_3}derived by solving Eq. (14).

2.3 Formulation of Wave Force

The wave pressure acting on the vertical circular cylinder is defined as follows:

$$P(x, y, z, t) = R_e\left[p(x, y, z) e^{-i\sigma t}\right] \tag{16}$$

The Bernoulli equation is used to get the pressure:

$$p = \rho g \frac{H}{2} \phi \tag{17}$$

where ρ is the water density.

The wave force in j direction acting on the cylinder mth is defined as follows:

$$F_j^m = R_e\left[f_j^m e^{-i\sigma t}\right] \tag{18}$$

where j is the force direction.

The wave force in j direction is presented by using Ψ_i, Ψ_s as follows:

$$f_j^m = \rho g \frac{H}{2} \frac{\cosh k(z+h)}{\cosh kh} \int_{S_{H_m}} (\Psi_i + \Psi_s) n_j ds \tag{19}$$

Finally, by integrating the wave force from Eq. (19) in the z direction, the force on the cylinder is defined as follows:

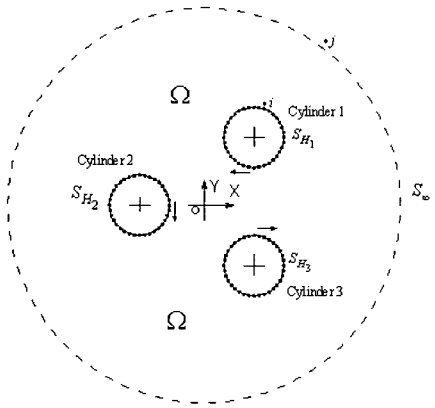

Fig. 2 Boundary discretization and the direction of numerical integration for calculating scattered wave potential.

$$f_j^m = \rho g \frac{H}{2} \frac{\tanh kh}{k} \int_{S_{H_m}} (\Psi_i + \Psi_s) n_j ds \tag{20}$$

where n_j is the normal vector in j direction, S_{H_m} is the boundary surface of the cylinder mth, m=1, 2, 3.

2.4 Formulation of Free Surface Elevation

The fluid region around the cylinders is taken for calculating free-surface elevation. The computation fluid region Ω is bounded by boundary of the cylinders S_{H_1}, S_{H_2}, S_{H_3} and the outside boundary S_B of the computation fluid region as shown in Fig. 3. Fig. 3 demonstrates the boundary discretization and the direction of numerical integration for calculating free-surface elevation.

The integral equation for the incident wave potential in the domain Ω as follows:

$$\Psi_i = \int_{S_{H_1}+S_{H_2}+S_{H_3}+S_B} \frac{\partial \Psi_i^e}{\partial n} G ds - \int_{S_{H_1}+S_{H_2}+S_{H_3}+S_B} \Psi_i^e \frac{\partial G}{\partial n} ds \tag{21}$$

where Ψ_i are the incident wave potential in the domain Ω. Ψ_i^e, $\frac{\partial \Psi_i^e}{\partial n}$ are the incident potential and the normal derivative of the incident wave potential on the boundary S_{H_1}, S_{H_2}, S_{H_3} and S_B . $G = -\frac{1}{2\pi} log r$ is the fundamental solution for Laplace equation.

The integral equation for the scattered wave potential in the domain Ω as follows:

$$\Psi_s = \int_{S_{H_1}+S_{H_2}+S_{H_3}+S_B} \frac{\partial \Psi_s^e}{\partial n} G ds - \int_{S_{H_1}+S_{H_2}+S_{H_3}+S_B} \Psi_s^e \frac{\partial G}{\partial n} ds \tag{22}$$

where Ψ_s are the scattered wave potential in the domain. Ψ_s^e, $\frac{\partial \Psi_s^e}{\partial n}$ are the scattered wave potential and the normal derivative of the scattered wave potential on the boundary S_{H_1}, S_{H_2}, S_{H_3} and S_B derived by solving Eq. (14) and Eq. (15). $G = \frac{i}{4} H_0^{(1)}(kr)$ is the fundamental solution for Helmholtz equation.

Once the incident wave potential and scattered wave potential are known then the total velocity potential ϕ can be calculated. The free-surface elevation η can be calculated from:

$$\eta = -\frac{1}{g} \left(\frac{\partial \phi}{\partial t} \right)_{z=0} \tag{23}$$

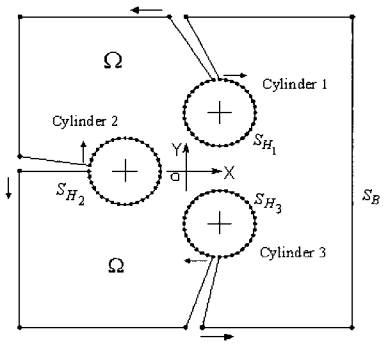

Fig. 3 Boundary discretization and the direction of numerical integration for calculating free-surface elevation.

3. Numerical Analysis and Remarks

Fig. 4 demonstrates the geometries of three cylinders in triangular array, column array and row array used in present study. The figure shows three cylinders having radius $a_1 = a_2 = a_3 = a$ subjected to incident wave comes from the left side. The maximum run-up is determined at point A, B, C on the cylinder 1, cylinder 2 and cylinder 3

respectively. The wave exciting forces on the cylinders and the free-surface elevation around the cylinders $10a$ distance are calculated.

Fig. 5 and Fig. 6 show the wave forces in x-direction and y- direction acting on cylinders in triangular array versus the wave number ka for the radius $a_1 = a_2 = a_3 = 1$, $h/a = 10$, and $D/a = 5$. The computed results of present study are strong agreement with those of Han and Ohkusu (1995).

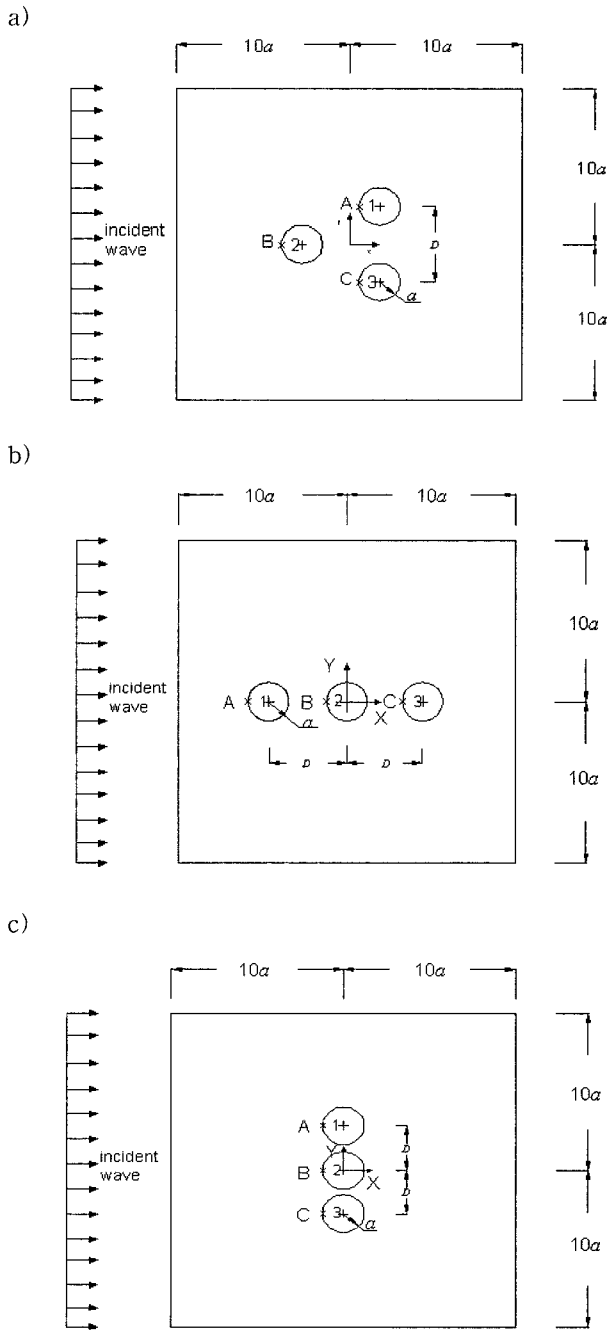

Fig. 4 Geometries for: (a) Triangular array, (b) Column array, (c) Row array

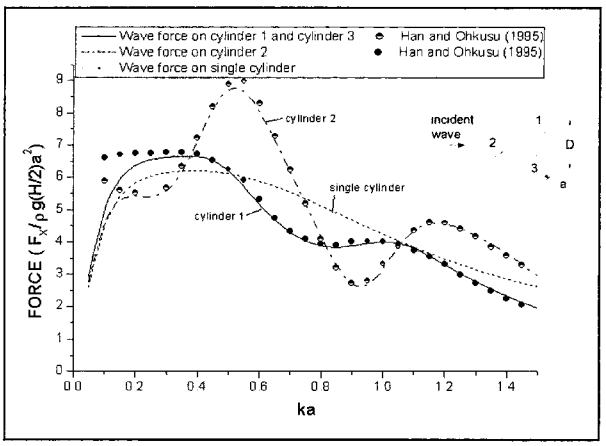

Fig. 5 Wave forces in x-direction versus wave number ka for radius $a_1 = a_2 = a_3 = 1$, $h/a = 10$, $D/a = 5$

Fig. 7 and Fig. 8 show the wave forces in x-direction acting on cylinders in triangular array versus the ratio $\gamma = 2a/D$ for the radius $a_1 = a_2 = a_3 = 1$ and $h/a = 10$. In this geometry, $\gamma = 1$ represents that the cylinders are touching each other, whereas $\gamma = 0$ means that the distance between two cylinder centers $D \to \infty$.

Fig. 9 shows the wave forces in y-direction acting on cylinder 1 and cylinder 3 in triangular array versus the ratio $\gamma = 2a/D$ for the radius $a_1 = a_2 = a_3 = 1$ and $h/a = 10$. To verify this method, the wave forces in x-direction and y -direction obtained in present study are compared with those of Chakrabarti (1978). The comparisons show that they are strong agreement.

Fig. 10 and Fig. 11 show the wave exciting forces in x-direction on cylinder 1 and cylinder 2 with the variation of incident wave angle $\beta = 0^o, 30^o, 45^o, 60^o$, respectively.

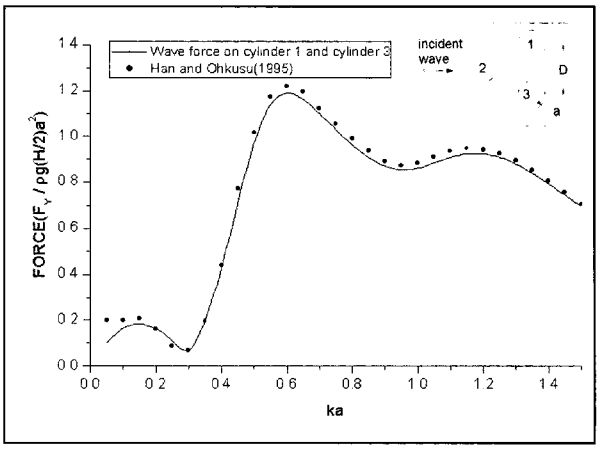

Fig. 6 Wave forces in y-direction acting on cylinder 1 and cylinder 3 versus wave number ka for radius $a_1 = a_2 = a_3 = 1$, $h/a = 10$, $D/a = 5$

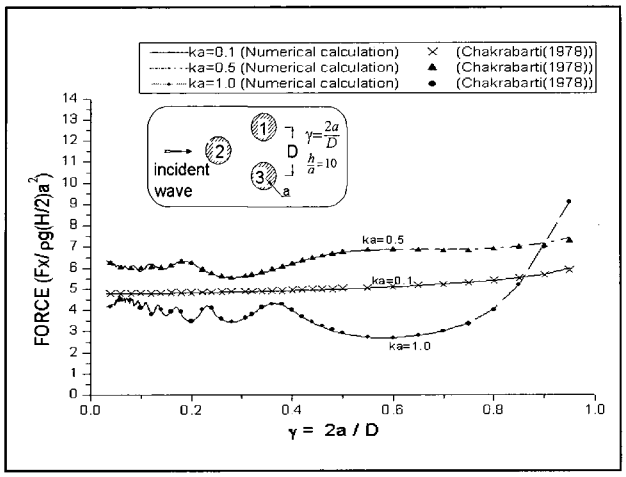

Fig. 7 Wave forces in x-direction acting on cylinder 1 and cylinder 3 versus ratio γ for radius $a_1 = a_2 = a_3 = 1,\ h/a = 10$

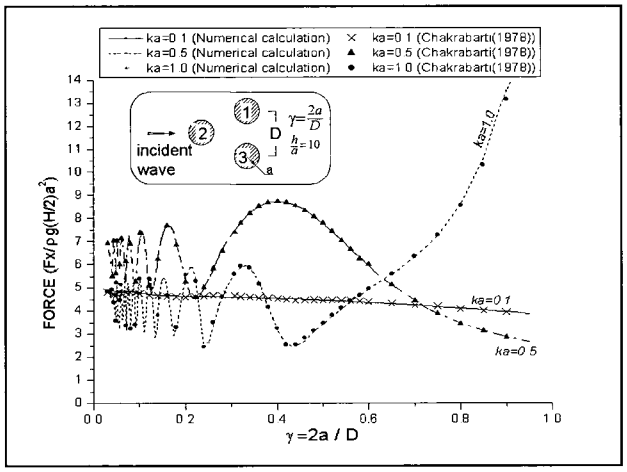

Fig. 8 Wave forces in x-direction acting on cylinder 2 versus ratio γ for radius $a_1 = a_2 = a_3 = 1,\ h/a = 10$

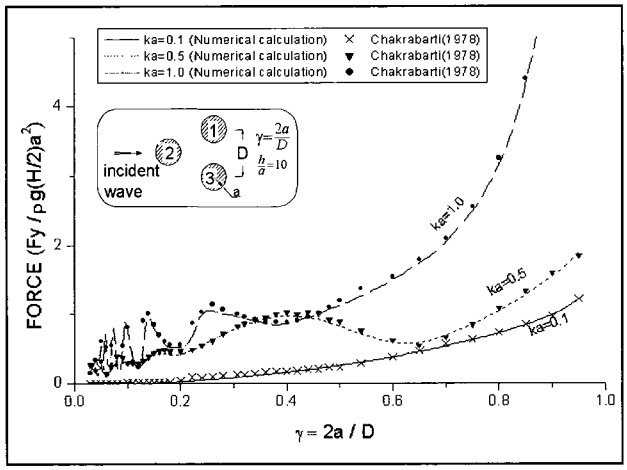

Fig. 9 Wave forces in y-direction acting on cylinder 1 and cylinder 3 versus ratio γ for radius $a_1 = a_2 = a_3 = 1,\ h/a = 10$

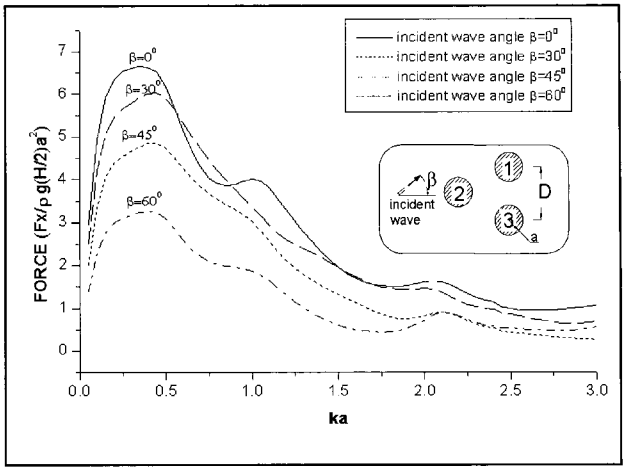

Fig. 10 Wave forces in x-direction on cylinder 1 versus the variation of incident wave angle for radius $a_1 = a_2 = a_3 = 1,\ h/a = 10,\ D/a = 10$

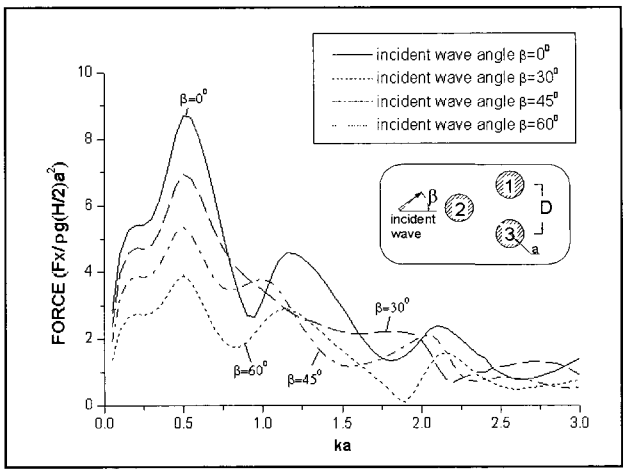

Fig. 11 Wave forces in x- direction on cylinder 2 versus the variation of incident wave angle for radius $a_1 = a_2 = a_3 = 1,\ h/a = 10,\ D/a = 10$

The wave forces acting on cylinders in row array are also investigated in present study. Fig. 12 and Fig. 13 show the wave forces in x-direction acting on cylinders in row array versus the ratio $\gamma = 2a/D$ for the radius $a_1 = a_2 = a_3 = 1$ and $h/a = 10$. The wave forces in x-direction on cylinders in column array versus the ratio $\gamma = 2a/D$ is shown in Fig. 14. It is shown that the wave forces acting on the cylinders reach the maximum value near $\gamma = 0.45$.

Fig. 15 shows the wave forces in x-direction acting on cylinders in column array versus the wave number ka for the radius $a_1 = a_2 = a_3 = 1,\ h/a = 10$, and $D/a = 5$. Fig. 15 shows that the wave force on each cylinder reaches the maximum values near $ka = 0.5$ and the maximum wave forces on cylinders in column array extremely higher than the maximum wave force on single cylinder.

Fig. 16, Fig. 17 and Fig. 18 show the maximum run-up at A, B and C on the cylinders in three different arrays versus the wave number ka.

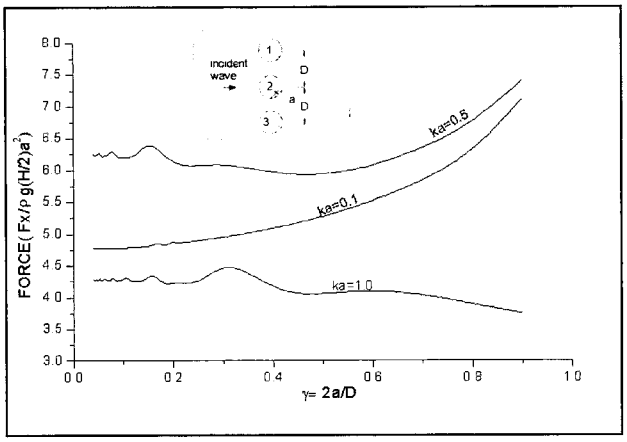

Fig. 12 Wave forces in x-direction acting on cylinder 1 and cylinder 3 versus ratio γ for radius $a_1 = a_2 = a_3 = 1$, $h/a = 10$

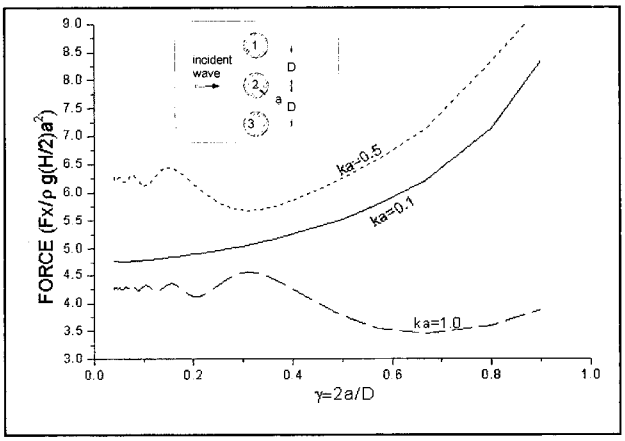

Fig. 13 Wave forces in x-direction acting on cylinder 2 versus ratio γ for radius $a_1 = a_2 = a_3 = 1$, $h/a = 10$

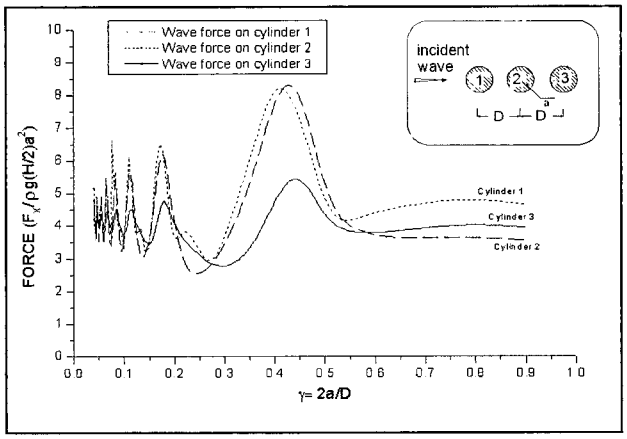

Fig. 14 Wave forces in x-direction acting on cylinders in column array versus ratio γ for radius $ka = 1$, $a_1 = a_2 = a_3 = 1$, $h/a = 10$

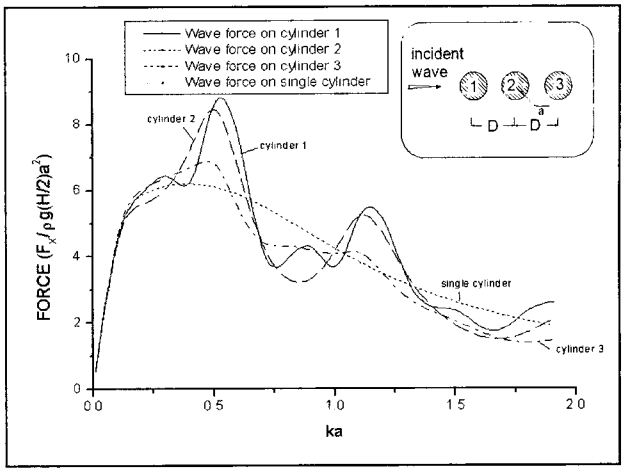

Fig. 15 Wave forces in x-direction acting on cylinders in column array versus wave number ka for radius $a_1 = a_2 = a_3 = 1$, $h/a = 10$, $D/a = 5$

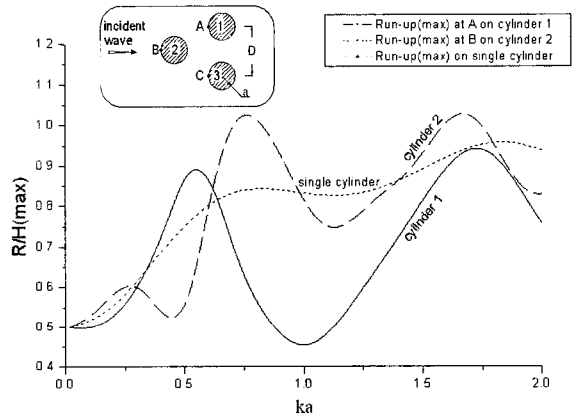

Fig. 16 Run-up at A and B on cylinder 1 and cylinder 2 in triangular array for $a_1 = a_2 = a_3 = 2$, $h/a = 5$, $D/a = 4$

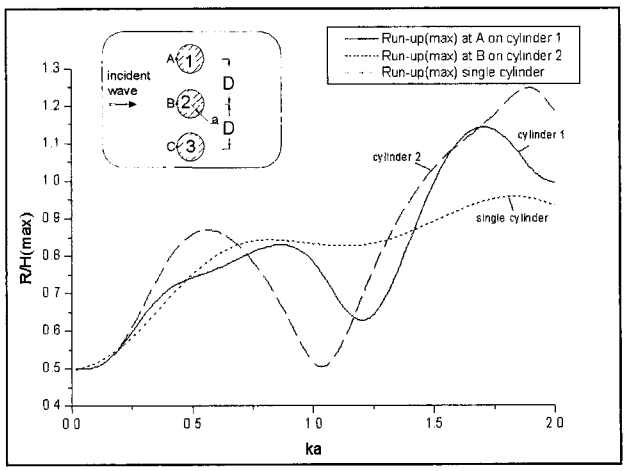

Fig. 17 Run-up at A and B on cylinder 1 and cylinder 2 in row array for $a_1 = a_2 = a_3 = 2$, $h/a = 5$, $D/a = 4$

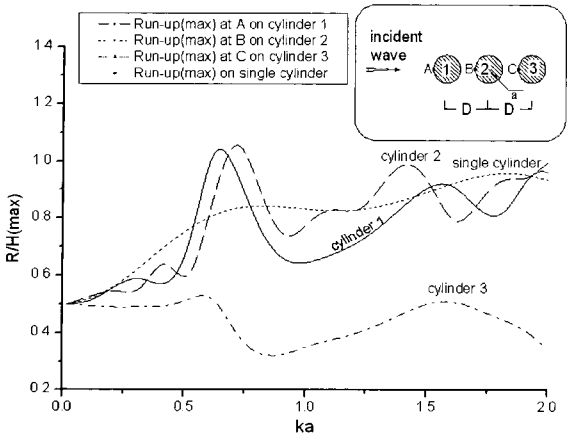

Fig. 18 Run-up at A, B, C on cylinders in column array for $a_1 = a_2 = a_3 = 2$, $h/a = 5$, $D/a = 4$

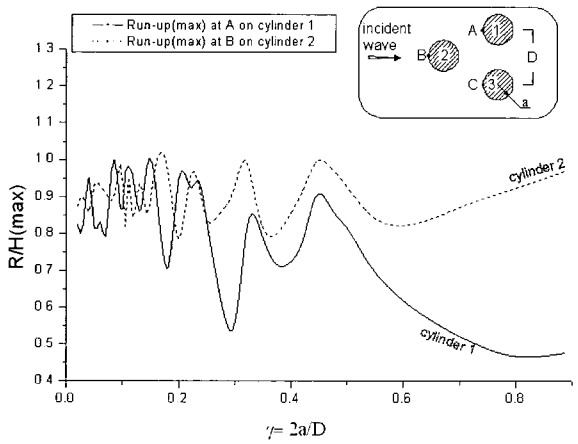

Fig. 19 Run-up at A, B on cylinder 1, cylinder 2 in triangular array versus ratio γ for $a_1 = a_2 = a_3 = 2$, $h/a = 5$, $D/a = 4$

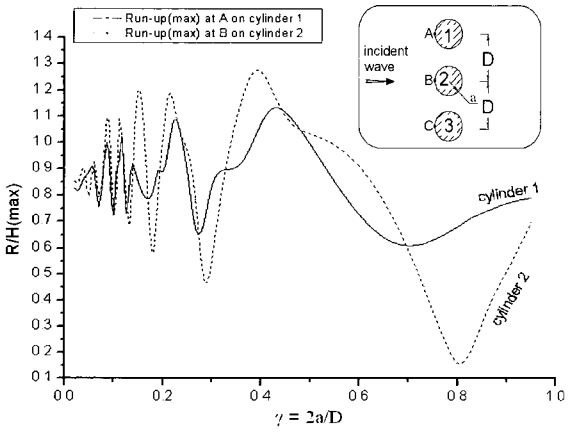

Fig. 20 Run-up at A, B on cylinder 1, cylinder 2 in row array versus ratio γ for $a_1 = a_2 = a_3 = 2$, $h/a = 5$, $D/a = 4$

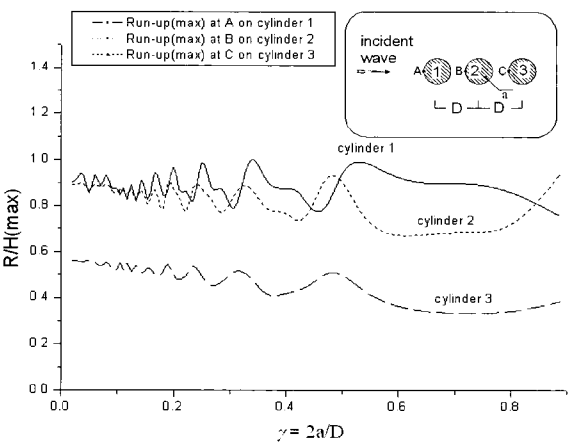

Fig. 21 Run-up at A, B, C on cylinders in row array versus ratio γ for $a_1 = a_2 = a_3 = 2$, $h/a = 5$, $D/a = 4$

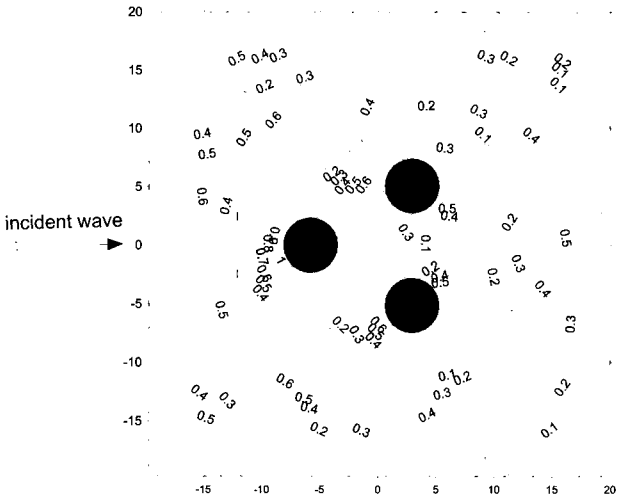

Fig. 22 Free-surface elevation contour around cylinders in triangular array for $a_1 = a_2 = a_3 = 2$, $h/a = 5$, $D/a = 5$

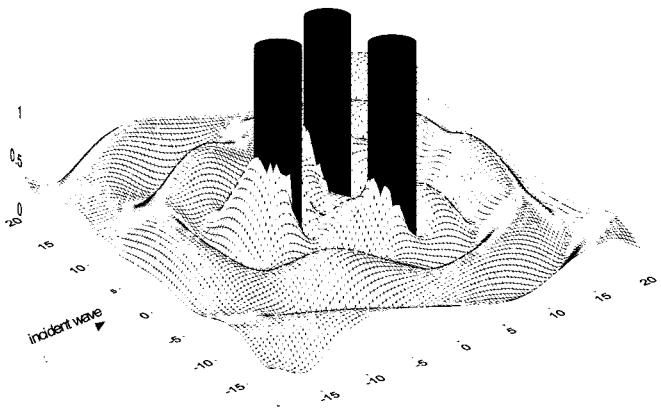

Fig. 23 Three-Dimensional free-surface elevation around cylinders in triangular array for $a_1 = a_2 = a_3 = 2$, $h/a = 5$, $D/a = 5$

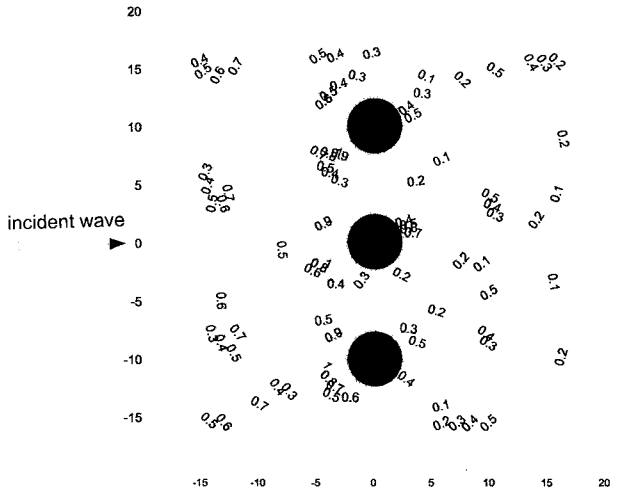

Fig. 24 Free-surface elevation contour around cylinders in row array for $a_1 = a_2 = a_3 = 2$, $h/a = 5$, $D/a = 5$

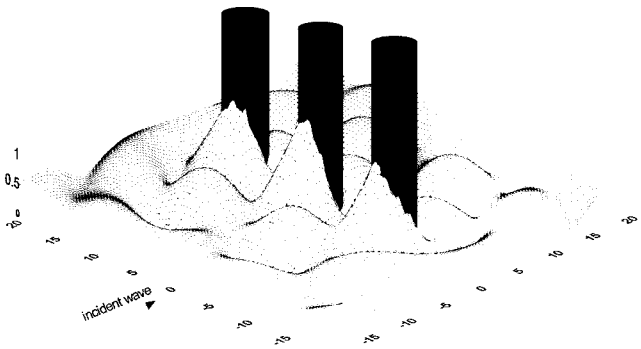

Fig. 25 Three-Dimensional free-surface elevation around cylinders in row array for $a_1 = a_2 = a_3 = 2$, $h/a = 5$, $D/a = 5$

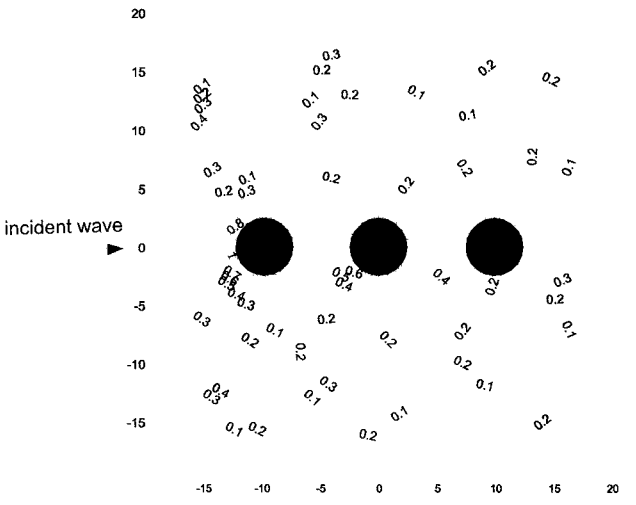

Fig. 26 Free-surface elevation contour around cylinders in column array for $a_1 = a_2 = a_3 = 2$, $h/a = 5$, $D/a = 5$

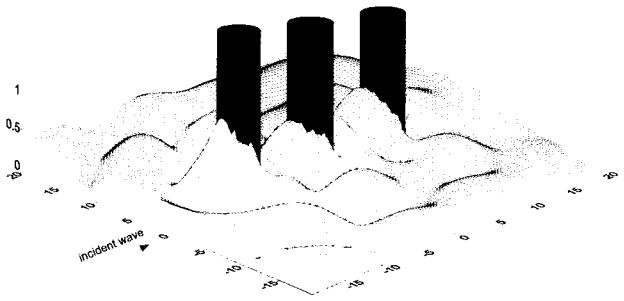

Fig. 27 Three-Dimensional free-surface elevation around cylinders in column array for $a_1 = a_2 = a_3 = 2$, $h/a = 5$, $D/a = 5$

Fig. 19, Fig. 20 and Fig. 21 show the maximum run-up at A, B and C on cylinders in three different arrays versus the ratio $\gamma = 2a/D$.

Also in this study, Fig.22 through Fig.27 show the free-surface elevations for three different arrays at $k = 0.75$, $D/a = 5$, $a_1 = a_2 = a_3 = 2$ and $h/a = 5$.

4. Conclusions

The wave forces acting on three vertical circular cylinders are analyzed by the boundary element method with Green's second theorem. To verify, the wave force results obtained in this study are compared with those of Han and Ohkusu (1995) and those computed by multiple scattering method (Chakrabarti, 1978). The comparisons show the excellent agreement between the results of this study and the results of them. Thus, the developed numerical analysis method with boundary element method is verified.

From the computed results, in column array, as the separated distance among the cylinders increases, the wave exciting forces on cylinders in column array reach the maximum value near $\gamma = 2a/D = 0.45$.

Also, the wave run-up on the cylinders in three different arrays are calculated. In column array, the maximum wave run-up on the back cylinder extremely lower than the maximum the maximum wave run-up on the front cylinder because of the shielding effect.

This numerical computation method will be used broadly in the design of vertical circular cylinders to be constructed in coastal zones in the future.

References

[1] Chakrabarti, S. K. (1978), "Wave forces on multiple vertical cylinders," Journal of Waterway, Port, Coastal

and Ocean Division, Vol. 104, No. 2, pp. 147-161.

[2] Chakrabarti, S. K. (2000), "Hydrodynamic interaction forces on multi-moduled structures," *Ocean Engineering*, Vol. 27, No. 10, pp. 1037-1063.

[3] Han, K. M. and Ohkusu, M. (1995), "Wave forces on groups of vertical circular cylinders," Research Papers, Ocean Resources Research Institute Dong-A University, Vol. 8, No. 1, pp. 17-26.

[4] Kagemoto, H. and Yue, D.K.P. (1986), "Interaction among multiple three-dimensional bodies in water waves," *Journal of Fluid Mech.*, Vol. 166, pp. 189-209.

[5] Kim, M. H. (1992), "Interaction of waves with N vertical circular cylinders," Journal of Waterway, Port, Coastal, and Ocean Engineering, ASCE Vol. 119, No. 6, pp. 671-689.

[6] Kim, N. H. and Park, M. S. (2007), "Wave force analysis of the vertical circular cylinder by boundary element method, KSCE Journal of Civil Engineering," Vol. 11, No. 1, pp. 31-35.

[7] Linton, C. M. and Evans, D. V.(1990), "The interaction of waves with arrays of vertical circular cylinders," *J. Fluid Mech.* No.46, pp.549-569.

[8] MacCamy, R. C. and Fuchs, R. A. (1954), "Wave forces on piles: a diffraction theory," Tech. Memo, No.69, US Army corps of Engineering, Beach Erosion Board.

[9] Spring, B. H. and Monkmeyer, P. L. (1974), "Interaction of plane waves with vertical cylinders," Proceedings of the fourteenth international conference on coastal engineering, Copenhagen, Denmark, ASCE, pp. 1828-1847.

[10] Williams, A. N. and Li. W. (2000), "Water wave interaction with an array of bottom-mounted surface-piercing porous cylinder," Ocean Engineering, Vol. 27, No. 8, pp. 841-866.

[11] Xianchu, Z., Dongjiao, W., and Chwang, A. T. (1997), "Hydrodynamic interaction between two vertical cylinders in water waves," *English Edition*, Vol. 18, No. 10.

Received 12 June 2008
Revised 10 September 2008
Accepted 24 September 2008